Characterization of a Narrow Channel to Study Flame Propagation and DDT

Yves Ballossier, Josué Melguizo-Gavilanes, Florent Virot
Institut Pprime, UPR 3346 CNRS, ISAE–ENSMA, BP 40109, 86961
Futuroscope Chasseneuil Cedex, France

1 Introduction

From a scientific point of view, Deflagration to Detonation Transition (DDT) continues to draw significant interest in the research community as an outstanding, physics-rich fundamental problem in combustion science. From a practical perspective, it is important to study and understand DDT in order to develop engineering correlations and simulation tools that can be applied to propulsion, and the prevention and mitigation of explosions. Reactive mixtures in confined geometries may detonate if ignited. Small flames can accelerate and undergo DDT, which, in most cases, presents significant safety hazards [1, 2], and, in others, can also be used to produce thrust or to generate power [3]. Understanding of the fundamental mechanisms of DDT continues to be a challenge in combustion theory. The specific details of DDT are dependent on many factors including channel geometry, size and blockage ratio [2]. Nonetheless, DDT, in general, proceeds through a series of distinct stages [2, 4]. Ignition of a deflagration drives a flow in the reactants and produces compression waves that propagate in front of the flame. This flow and the resulting turbulence stretches the flame and increases its surface area, which, in turn, accelerates the flame further. Eventually, compression waves generated by the accelerating flame coalesce to produce a precursor shock. In obstructed channels with large cross-sections ($\mathcal{O}(\text{cm})$ to $\mathcal{O}(\text{m})$) is relatively well established that transition to detonation occurs upon multiple reflections of the aforementioned precursor shock. In unobstructed channels with narrow cross-sections ($\mathcal{O}(\text{mm})$) however, feedback between the accelerating flame and shock compression is believed to subsequently ignite the gas and initiate a detonation. The exact DDT mechanisms for the latter length scale requires further study as boundary layer effects may play an important role in every stage of the DDT process. Here, we present the first step of the characterization of a new combustion channel that will systematically be improved to be able to focus on the different stages of DDT separately. Specifically, we focus on the effect of the ignition source and the extent of gas present between the ignition location and the closed-end of the channel (i.e. dead volume) on the early stages of flame propagation.

2 Experimental setup and procedure

A 10 mm $\times$ 10 mm (close-open end) square cross-section channel was machined on an aluminum block, and a sheet of polycarbonate, 8 mm thick, was bolted as the fourth side of the channel to allow optical access

Correspondence to: yves.ballossier@ensma.fr

for direct observation (see Fig. 1 – top). Electrodes are separated by 2 mm and located near the inlet (14 mm from the close-end). The effective channel length is 449 mm from the ignition point to the open end.

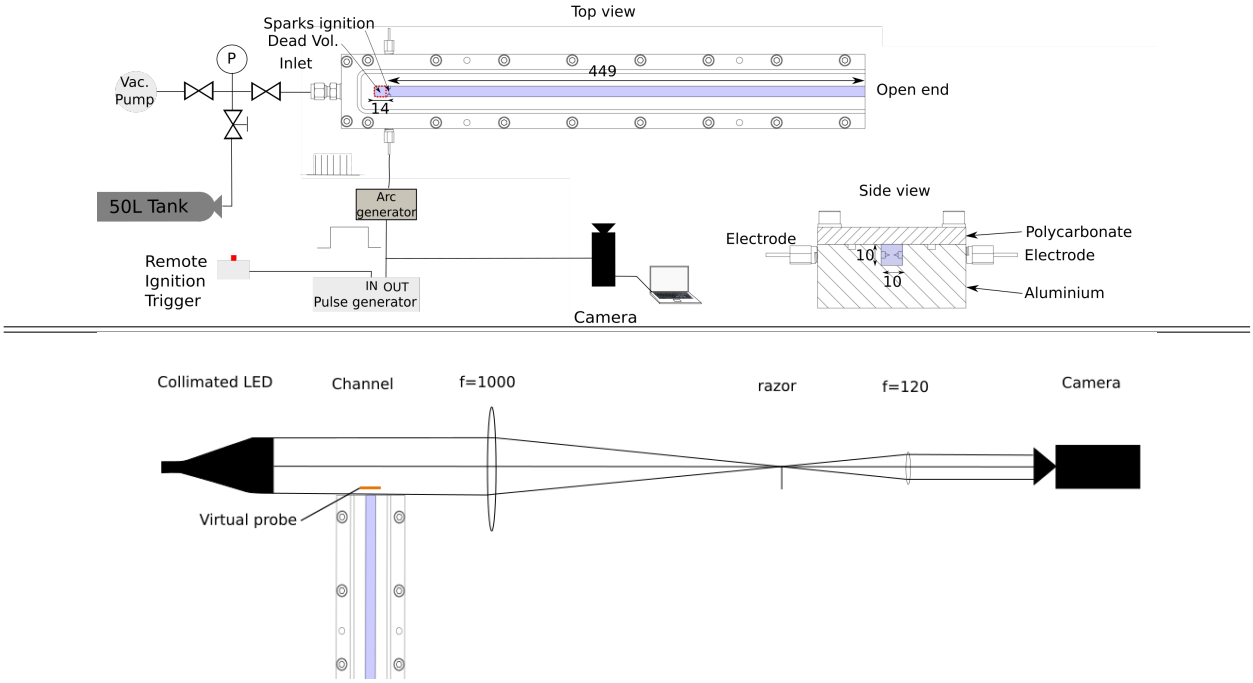

Figure 1: Schematic of experimental setup (top) and schlieren visualization system at channel exit (bottom).

For each experiment, the channel was vacuumed to an absolute pressure below 1 mbar (controlled by a MKS 220DA pressure sensor). A plastic cap sealed the open end of the channel. Subsequently, the reactive mixture (stoichiometric H_2-Air), prepared in an external tank (50 L bottle) using the method of partial pressure, was fed into the channel up to atmospheric pressure. At this point, the plastic cap was no longer attached to the channel and was removed. This procedure ensured adequate control of the mixture composition.

Ignition was achieved using an electric lighter connected to two electrodes; a signal was transmitted to an arc generator operated at a frequency of about 16 kHz, determined with the camera described below set at 200 kHz, and crossed-checked with both current (Lecroy AP015) and voltage (Tektronix P6015A) probes. From these measurements the electric energy computed was approximately 0.02 mJ per arc. The arc generator frequency was kept fixed and the number of arcs was controlled by varying the length of time the arc generator was active. The ignition and subsequent flame propagation inside the channel was visualized directly using a black and white Photron FASTCAM SA-Z equipped with a Sigma 17-50 mm objective. The frame rate chosen (10,000 fps) allowed to visualize the entire channel at a spatial resolution of 1024 $\times$ 24 pixels (about 0.45 mm/pixel). The same trigger was used for the camera and arc generator to synchronize the data acquisition. Schlieren visualization at the end the channel was performed using an in-line configuration with the same camera described above. The setup included a 100 mm collimated white LED, and two BK7 lenses of 150 mm and 50.8 mm diameter with focal lengths of 1000 mm and 120 mm, respectively. Cut-off was handled using a razor blade positioned at 45° set to block about 50 % of the light beam. Videos were recorded at 75 kHz with an exposure of 347 ns. The image resolution was set to 640 $\times$ 376 pixels. A schematic of the schlieren set up is shown in Fig.1 – bottom.

In an attempt to understand the influence of the ignition source and the existence of a dead volume behind the electrodes on early stages of flame propagation, we varied both variables independently: the number of arcs during ignition between 6 and 287 (resulting in a total electric energy deposit of 0.12 mJ and 5.7 mJ, respectively), and added a removable plastic insert of 11 mm $\times$ 10 mm $\times$ 10 mm behind the electrodes. For each experimental condition, at least three tests were conducted to assess repeatability.

3 Results and Discussion

Experiments were performed with stoichiometric H_2-Air mixtures at room conditions, around $p_0 = 100$ kPa, and T_0 = 290 K. Direct observation of flame propagation from the ignition point ($x = 0$ mm) to the outlet of the channel are presented on an $x - t$ diagram in Fig. 2 to assess the effect of the number of arcs.

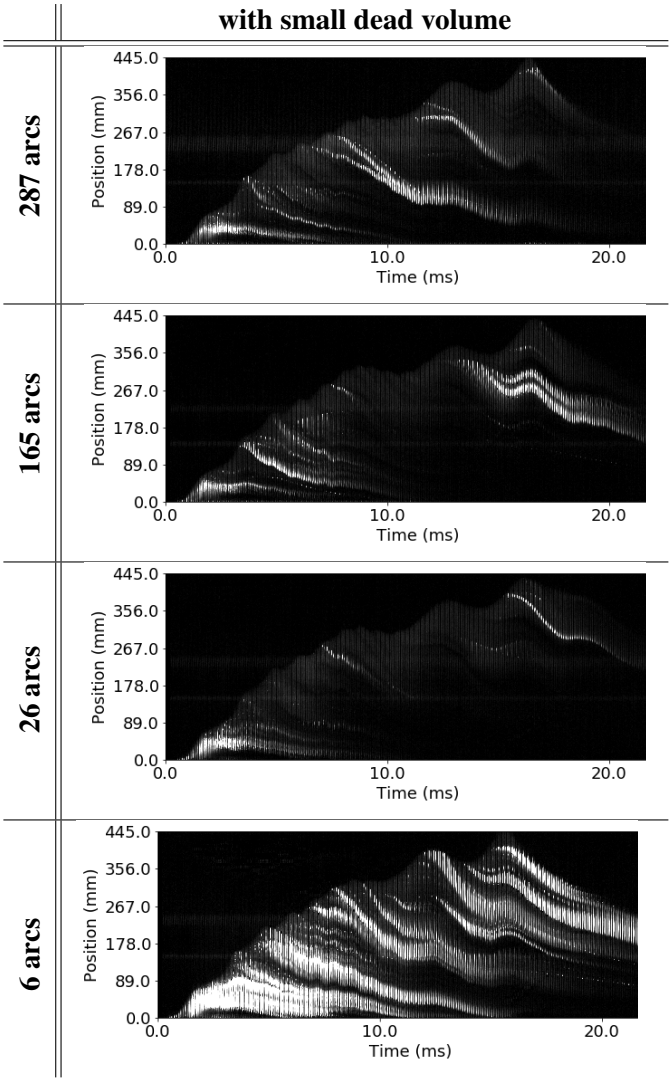

Figure 2: $x - t$ diagram for an accelerating H_2-Air flame propagating at varying arcs number using direct observation. Configuration: small dead volume.

The raw images were enhanced by applying Gaussian denoising and contrast adjustment using standard image postprocessing software. Each $x - t$ diagram exhibits emission of light at varying intensities in the combustion products. At around 15.5 ms, the luminous front reaches the end of the channel in most cases. The visible emission after this point comes from the burned gas that remains inside the channel.

The luminous oscillations noticeable in the Fig. 2 arise from flame-acoustic wave interactions. Preliminary analyses of the acoustic time scales present in our facility, $\tau_{\text{acous}} = L/c$, support this statement. To investigate the aforementioned flame-acoustic interactions further, we performed schlieren at the channel exit. As the flame accelerates in the channel, pressure waves emanating from the flame front travel upstream towards the open-end. These waves manifest themselves at the channel exit as visible puffs of fresh reactive mixture whose frequency can be quantified by placing a virtual line probe (see Fig. 1 – bottom). At each frame from the schlieren videos, the background was subtracted, and the mean light intensity over the probe was computed and recorded to reconstruct the puffing time history. A sample case for a small dead volume and 165 arcs is shown in Fig. 3. Note that the mean intensity was normalized using the maximum value recorded over the entire evolution. Red squares are visual indicators of puffs observed prior to the arrival of the flame at the channel exit, indicated by a dashed vertical line. While there are slight discrepancies regarding the times the puffs are observed, the number of puffs recorded is consistent with the oscillations seen in Fig. 2. Some of our tests showed that the flame does not always reach the end of the channel suggesting that expansions traveling back into the channel upon arrival of the puffs are sometimes strong enough to quench the flame. We plan to investigate this behavior in future work. Qi et al. [5] also used schlieren in a similar configuration but to characterize the external flow field.

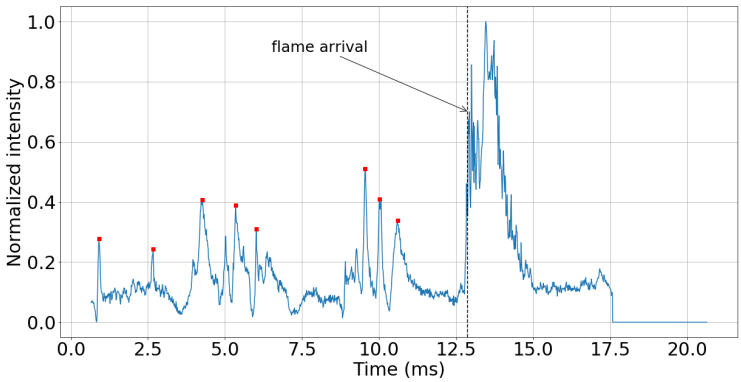

Figure 3: Puffs time history for small dead volume and 165 arcs. Red squares indicate the pulses due to the puffs across the virtual probe; the black dashed line indicates the flame arrival time.

Liveing and Dewar [6] showed that radiation from hydrogen-oxygen flames increases with pressure, hence the re-illumination oscillations observed behind the flame could be caused by a pressure increase during flame acceleration. Results show imperceptible differences in the flame evolution as a function of number of arcs for $t < 10$ ms. Note that in the current results, direct observation does not allow to visualize the presence of OH in the reaction zone of the flame because the polycarbonate sheet filters the wavelength at which spontaneous emission of OH occurs (308 nm). Available literature data on spectrometry suggests that the emission bands present in our results come from the vibration-rotational spectrum of water, which lies in the visible spectrum [7, 8]. Additionally, Schefer et al. [9] demonstrated that an increase in temperature only

leads to an emission intensity increase without influencing the spectral structure of the gas. Consequently, the spontaneous emission captured by the camera gives a slightly lower estimation of the true reactive front speed. From here on, *front position*, corresponds to the visible emission captured by the camera.

In Fig. 4, $x-t$ diagrams show the effect of the presence of dead volume on the luminous front as a function of numbers of arcs. The presence of a dead volume behind the electrodes seems to have a perceptible effect on flame propagation. Having a large dead volume allows the flame to propagate towards the close-end causing the front that propagates towards the open-end to be affected by the expansion of burned gases. The luminous front reaches the end of the channel at around $t = 8$ ms, 52% faster than the case with small dead volume. Our results are also consistent with the observations in [10, 11]. They showed that the initial stage of flame propagation is independent of acoustics. Indeed, curves with large and small dead volume in Fig. 5, match during the first millisecond.

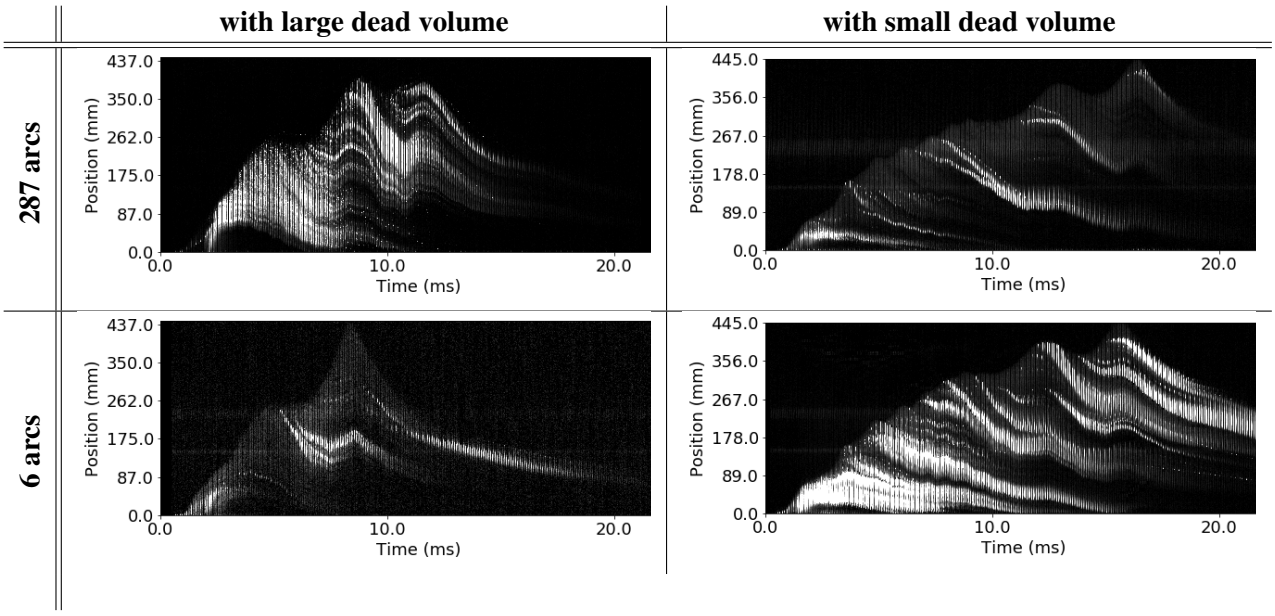

Figure 4: Comparison of selected $x-t$ diagrams for accelerating H_2-Air flames using direct observation.

Fig. 5 gathers all our experimental results (25 shots with small and large dead volume including all number of arcs tested). The front was automatically detected using a postprocessing script written in Python. The luminous signals were averaged over the height of the channel and the peak of luminous intensity tracked. Red and blue symbols represent cases with small and large dead volume. Overall, results show reasonable repeatability. There are minor differences for each configuration during the first 10 ms of propagation. The front position is fitted to a second order polynomial, then analytically differentiated to obtain corresponding velocities and accelerations. For the case with small dead volume, the front evolution is more regular, even if front fluctuations are present. The initial front velocity, 0 ms $< t <$ 4 ms, was computed to be 45 m/s and 60 m/s for small and large dead volume, respectively. The flame arrival times were dependent on the presence of dead volume but independent of the number of arcs used, they varied from 8 ms (large dead volume) to 12 ms / 15.5 ms (small dead volume). As mentioned above, in some cases the flame did not reach the end of the channel.

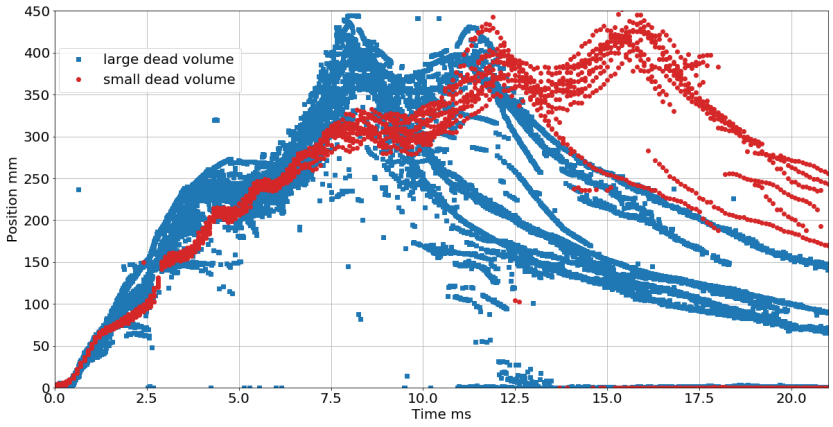

Figure 5: Luminous front position as a function of time for all experiments performed (25 shots) including all number of arcs tested. Blue symbols: 14 shots; red symbols: 11 shots.

4 Conclusion and perspectives

Stoichiometric H_2-Air flame propagation experiments were conducted using a 10 mm $\times$ 10 mm square cross-section channel of 449 mm in length. The effect of ignition source and the presence of a dead volume behind the electrodes on flame propagation was assessed. Results show that the number of arcs have a negligible impact on the overall evolution, while the presence of a dead volume has a noticeable effect. A test performed (not shown here) using a stoichiometric H_2-O_2 resulted in DDT in our channel. Similar to our results, research in [10–14] showed the flame-acoustic interactions induced by an oscillating flame front. Here, using schlieren at the end of the channel, we demonstrate that these oscillations/puffs result in an inflow of air that changes the mixture composition in the last portion of the channel. This could explain some of the variability observed in our results under the same test conditions. Particularly, the quenching of the flame before reaching the exit. Future work will include extending the range of conditions tested (i.e. less diluted H_2-Air mixtures), as well as improved visualization of the flame evolution inside the channel.

Acknowledgement: This work was supported by the CPER FEDER Project of Région Nouvelle Aquitaine.

References

[1] R. Zipf Jr, V. Gamezo, M. Sapko, W. Marchewka, K. Mohamed, E. Oran, D. Kessler, E. Weiss, J. Addis, F. Karnack *et al.*, "Methane–air detonation experiments at niosh lake lynn laboratory," *Journal of Loss Prevention in the Process Industries*, vol. 26, no. 2, pp. 295–301, 2013.

[2] G. Ciccarelli and S. Dorofeev, "Flame acceleration and transition to detonation in ducts," *Progress in energy and combustion science*, vol. 34, no. 4, pp. 499–550, 2008.

[3] P. Wolański, "Detonative propulsion," *Proceedings of the combustion Institute*, vol. 34, no. 1, pp. 125–158, 2013.

[4] M. Liberman, M. Ivanov, A. Kiverin, M. Kuznetsov, A. Chukalovsky, and T. Rakhimova, "Deflagration-to-detonation transition in highly reactive combustible mixtures," *Acta Astronautica*, vol. 67, no. 7-8, pp. 688–701, 2010.

[5] S. Qi, Y. Du, P. Zhang, G. Li, S. Wang, Y. Li, and T. Dong, "Experimental study of gasoline vapor deflagration in a duct with an open end," *Combustion and Flame*, vol. 193, pp. 16–24, 2018.

[6] G. Liveing and J. Dewar, "On the influence of pressure on the spectra of flames," *Astronomy and Astro-Physics (formerly The Sidereal Messenger)*, vol. 11, pp. 215–223, 1892.

[7] T. Kitagawa, "Emission spectrum of the oxy-hydrogen flame and its reaction mechanism:(i) formation of the activated water molecule in higher vibrational states," *The Review of Physical Chemistry of Japan*, vol. 13f, no. 2, 1939.

[8] A. G. Gaydon, "Flame spectra in the photographic infra-red," *Proceedings of the Royal Society of London. Series A. Mathematical and Physical Sciences*, vol. 181, no. 985, pp. 197–209, 1942.

[9] R. W. Schefer, W. D. Kulatilaka, B. D. Patterson, and T. B. Settersten, "Visible emission of hydrogen flames," *Combustion and flame*, vol. 156, no. 6, pp. 1234–1241, 2009.

[10] S. Kerampran, D. Desbordes, and B. Veyssiere, "Study of the mechanisms of flame acceleration in a tube of constant cross section," *Combustion science and technology*, vol. 158, no. 1, pp. 71–91, 2000.

[11] S. Kerampran, D. Desbordes, B. Veyssière, and L. Bauwens, "Flame propagation in a tube from closed to open end," in *39th Aerospace Sciences Meeting and Exhibit*, 2001, p. 1082.

[12] H. Guenoche, "Flame propagation in tubes and in closed vessels," in *AGARDograph*. Elsevier, 1964, vol. 75, pp. 107–181.

[13] J. Gray, J. P. Moeck, and C. O. Paschereit, "Flame propagation from the closed end of an open-ended tube: an analysis of the effects of fuel type, tube length, and equivalence ratio and an insight into flame dynamics," in *49th AIAA/ASME/SAE/ASEE Joint PropulsionConference*, 2013, p. 3656.

[14] F. F. Fachini and L. Bauwens, "Oscillatory flame propagation: Coupling with the acoustic field," *Proceedings of the Combustion Institute*, vol. 34, no. 2, pp. 2043–2048, 2013.